Mechanics & Industry **16**, 208 (2015)

DOI: 10.1051/meca/2014086
www.mechanics-industry.org

Mechanics & Industry

Design and characterization of an assembly to obtain a linkage pivot by crimping process

Moncef Hbaieb, Ahmed Kacem and Abdelkader Krichen[a]

Laboratoire de Génie de Production Mécanique et Matériaux, National Engineering School of Sfax, University of Sfax, B.P. 1173, 3038 Sfax, Tunisia

Received 26 June 2013, Accepted 11 December 2013

Abstract – The purpose of this research is to design and test a linkage pivot assembled by metal forming process. The assembly is obtained by crimping a tubular component onto a cylindrical grooved component using an experimental instrumented device. The quality of the linkage pivot is evaluated by a pullout test which measures the force required to break or dismantle the assembly. The study is focused on analysing the effect of the main process parameter (i.e. the crimping depth) and geometrical parameters (i.e. the tubular component thickness and the groove radius). For one set of geometrical parameters, an appropriate crimping depth leading to the maximum assembly strength and assembly stiffness is determined. The study of the geometrical parameters shows that the tubular component thickness and the groove radius do not affect much the assembly strength. However, the tubular component thickness affects considerably the forming load, the assembly stiffness and the failure mode. According to the obtained results, one set of parameters that meets industrial requirements is selected to design the linkage pivot.

Key words: Metal forming / crimping / assembly / linkage pivot / pullout test

1 Introduction

In recent years, a growing interest in mechanical assembly operations is set to reduce additional components such as screws, pegs, rivets, pins, spurs, bolts and nuts. Consequently, assemblies obtained by metal forming processes have been widely used in mechanical design [1, 2]. For several applications, clinching and hemming are the possible alternatives [3,4]. Particularly for tubular components, crimping is the most popular of the metal forming processes used to obtain a mechanical assembly such as the fixed joint.

In the literature, several researchers have done much work on joining tubular components by crimping process. Shirgaokar et al. [5] studied the effect of various process variables to optimize the process so that the effect of springback could be reduced and the assembly quality, as indicated by the pullout force, could be improved. By another work, Shirgaokar et al. [6] investigated the crimping process using a polyurethane tool and hydraulic pressure to enhance the performance of the assembly by determining the optimum process and geometrical parameters. In these two studies, the analysed parameters are the geometry, alignment and stroke of the crimper, friction, material properties and also manufacturing errors. Recently, Fresnel et al. [7] studied the structural response of the airbag inflator tubes from the crimping to destructive burst test stages. It was found that the numerical damage maps obtained after the crimping process and during the burst tests are in good agreement with the experimental data. On the other hand, Park et al. [8] performed finite element simulations and strength tests in order to design an axial joint and a torque joint made by the electromagnetic forming which is described by Psyk et al. [9]. The authors concluded that multiple grooves with different radii or depths should be combined in the design of the crimped region to manufacture a link according to the desired strength.

The present study deals with obtaining an assembly between two cylindrical rods without the use of additional components. The assembly is obtained by crimping the end of a tubular rod onto the end of a grooved rod. In this work, the aim of the crimping process is not to obtain a fixed joint as the case of the major previous works, but rather to obtain a revolute joint. Crimping process is performed by means of an experimental instrumented device in order to determine the forming load. To make sure of the final performance and the safety of the linkage, the maximum pullout force during a destructive testing

[a] Corresponding author: krichenabdelkader@yahoo.fr

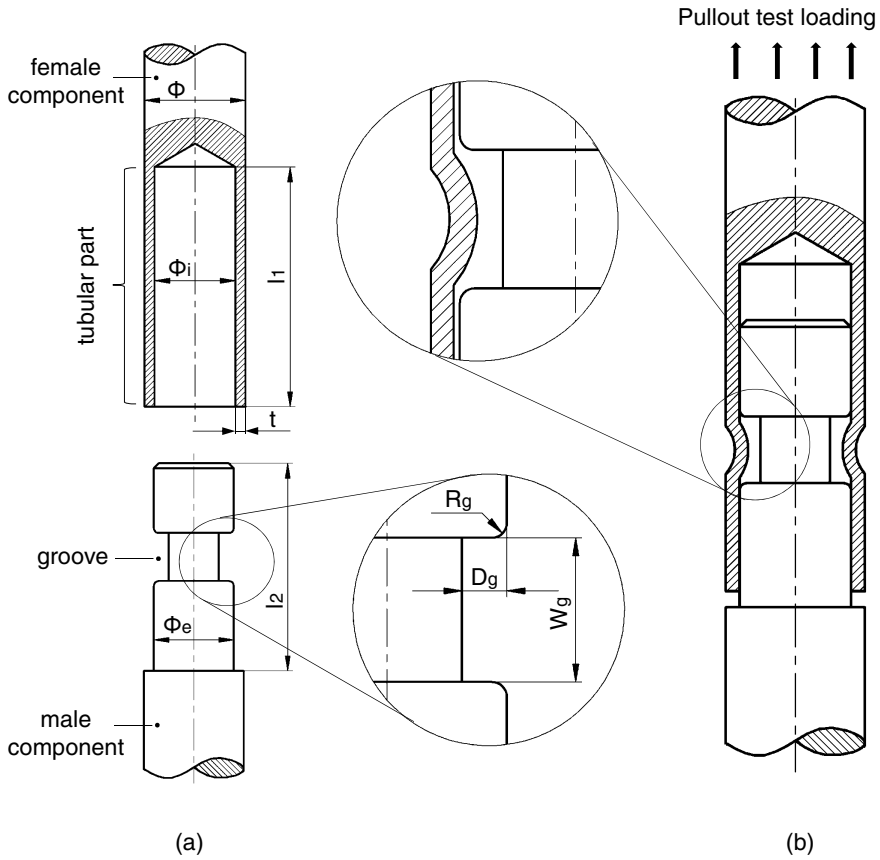

Fig. 1. Assembly components: (a) before crimping (b) after crimping.

phase is analysed. Several assemblies with various sets of process and geometrical parameters are tested to find the appropriate values that meet some performance and industrial requirements.

2 Experiments

2.1 Assembly components

To obtain an assembly by crimping, a female component and a male component were designed as shown in Figure 1. The female component has an inner diameter of ϕ_{i}, a wall thickness of t and an axial length of l_1 as shown in Figure 1a. The male component, designed with a groove, has a ϕ_e outer diameter and a l_2 axial length. The geometrical parameters of the groove are the groove width W_{g}, the groove depth D_{g} and the groove radius R_{g}.

The boring of the female component which has the inner diameter ϕ_{i} and the male component which has the outer diameter ϕ_e were designed with the same nominal diameter ϕ_{n}. With a view to obtain a linkage pivot, they were designed to fit together with a clearance value set to 0.1 mm.

From an economical point of view, the increase of the groove width W_{g} and the groove depth D_{g} is needless. The increase of these two parameters causes the increase of manufacturing cost. In this work, W_{g} and D_{g} were minimized and were set to their lower limits as indicated in Table 1. Accordingly, the effect of only two geometrical parameters (t and R_{g}) was studied, while keeping constant the other parameters. The nomenclature of the geometrical parameters and the considered values are summarized in Table 1.

A commercial brass rod was used as the component linkage material. Uniaxial tensile test was used to describe the stress-strain relationship. The tensile tests were carried out on bone-shaped specimens with a diameter of 6 mm and a gauge length of 50 mm. The tests were performed under displacement control at a constant rate of 5 mm.min^{-1}. The true stress was calculated by the ratio of the load over the current section of the sample. The current section was determined from the initial section of the sample by assuming both isochoric plastic deformation and a homogeneous distribution of strain along the gauge length of the sample. The true strain is equal to the natural logarithm of the ratio of length at any instant to original length. Figure 2 shows the obtained stress-strain curve. The mechanical properties determined from these tests are shown in Table 2.

To manufacture the female and male components, two parts were cut from a commercial brass cylindrical rod with a diameter of $\phi = 10$ mm. Only one end of each part was machined using a computerized numerical control (CNC) lathe. The tubular part of the female component

Table 1. Geometrical parameters of the assembly.

Nomenclature	Symbol	Considered values (mm)
Rod diameter	ϕ	10
Nominal diameter	ϕ_n	8–8.5
Wall thickness	t	1–0.75
Female component length	l_1	26
Male component length	l_2	20.8
Groove width	W_g	4.8
Groove depth	D_g	1.5
Groove radius	R_g	0–0.2–0.5–1

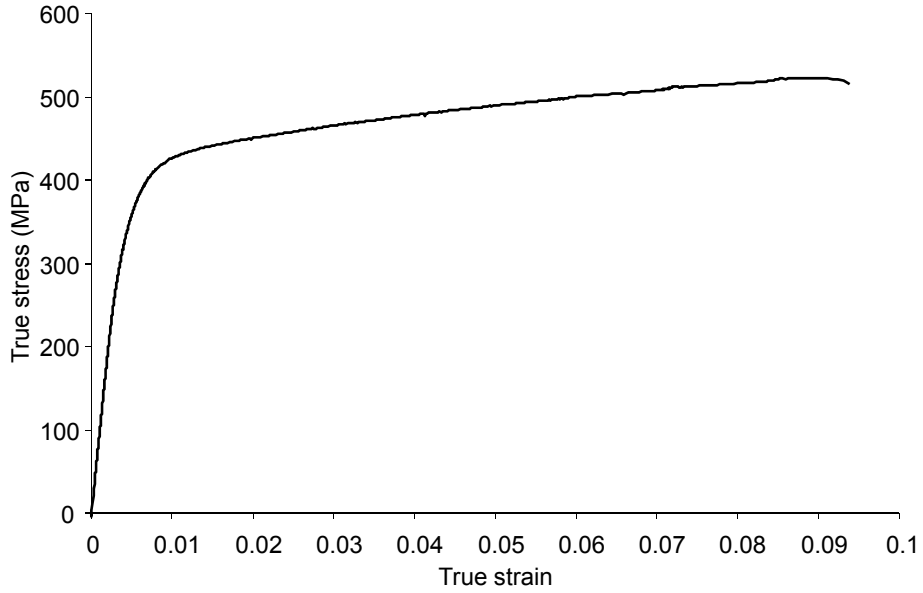

Fig. 2. Stress-strain curve.

Table 2. Mechanical properties of the brass rod.

Young's modulus (GPa)	96
0.2% yield stress (MPa)	385
Strength coefficient K (MPa)	644
Strain-hardening exponent n	0.087

was manufactured by drilling operation preceded by a center-drilling operation to obtain a hole precisely centered in the cylindrical rod. The male component was machined by turning and grooving operations.

2.2 Assembly procedure

The technique used to assemble the male and female components by crimping consists of pushing partially the tubular part into the groove as shown in Figure 3. This operation was performed by applying firstly a local deformation on the female component using a narrow roller tool and then rotating the female component so as to deform the workpiece along a circular path. To achieve the desired shape, these actions were repeated until reaching the required value of the crimping depth P_c as shown in Figure 3. To prevent components bending during forming, a cylinder was mounted in the opposite side of the roller tool. Note that, both the roller tool and the opposite cylinder were free to rotate about their axis. In addition to t and R_g, the crimping depth P_c was counted as a process parameter to be also studied. The considered values of P_c are 0.6, 0.8, 1 and 1.2.

A specific instrumented device was manufactured for crimping as shown in Figure 4. This device was equipped with a displacement gauge and a load cell to measure the roller tool displacement p and the opposite cylinder reaction R, respectively. The experimental procedure of crimping was performed as follows. Firstly, a good alignment between the roller tool and the groove was set. Secondly, the male component was inserted into the female component until its shoulder. Thirdly, a local deformation of the female component was induced by applying a displacement increment Δp to the roller tool by a lead-screw that induced also a reaction force increment ΔR. This stage was performed under reaction force control at a constant increment $\Delta R = 0.1$ kN. Fourthly, a single rotation was applied to the female component by a handwheel to deform the workpiece along a circular path. The third and the forth stages were repeated in the same manner until the imposed displacement reached progressively the required value of the crimping depth P_c. The values of P_c

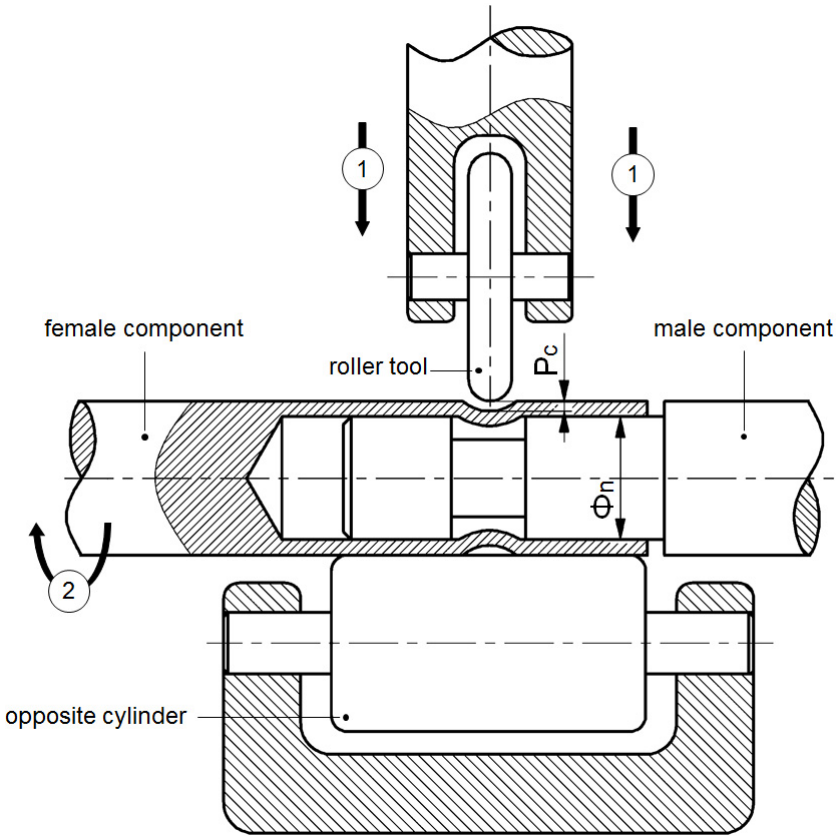

Fig. 3. The crimping process.

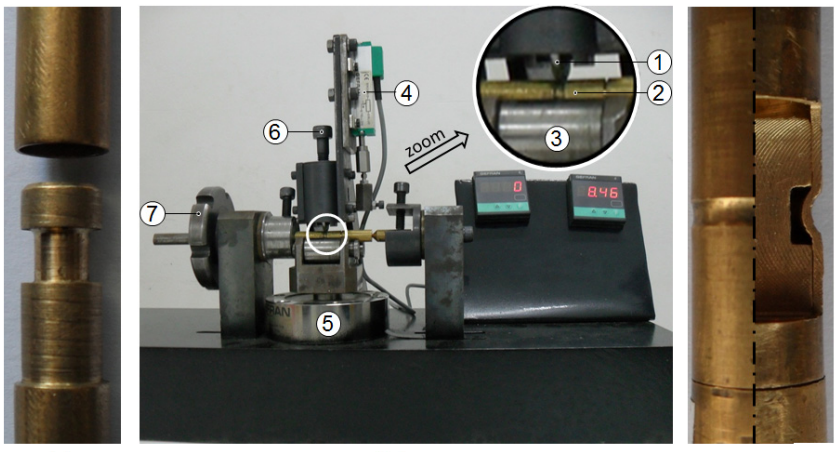

Fig. 4. (a) Components before crimping, (b) experimental device: (1) roller tool, (2) workpiece, (3) opposite cylinder, (4) displacement gauge, (5) load cell, (6) leadscrew and (7) handwheel and (c) components after crimping.

were set in such a way to not constraint completely the assembly. Figure 4 shows a typical example of the manufactured components, the experimental device of crimping and an actual half section view of the obtained assembly.

2.3 Pullout test

To analyse the maximum assembly strength after crimping, the assembly was subjected to a pullout test. The male component was totally embedded while an uniaxial tension was applied to the female component until failure as shown in Figure 1b. This destructive test was performed to check the minimum limit value stipulated by a local industry aimed at producing a strong assembly that bears heavy external loading.

The pullout test was carried out with a universal traction-compression testing machine of maximum load 50 kN. It was performed under displacement control at

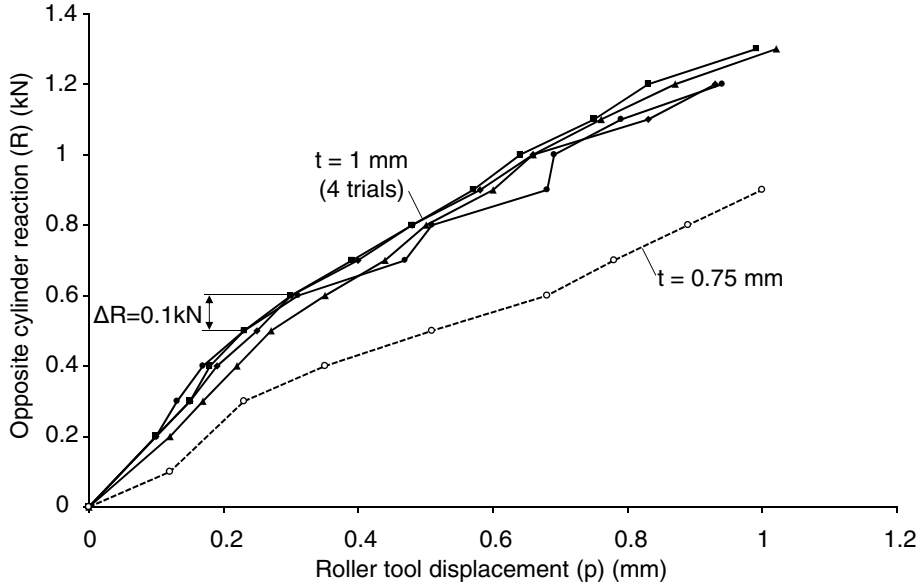

Fig. 5. The opposite cylinder reaction versus the roller tool displacement.

a constant low rate of 5 mm.min^{-1}. The outputs of the displacement gauge and the load cell were continuously stored in a data acquisition system.

3 Results and discussion

3.1 Process validation

After crimping, it was usually found that the female part is free to rotate around the male part. Thus, as excepted, a linkage pivot and not a fixed joint was obtained in all cases. It was also found that the desired geometry is achieved without defects. To illustrate the final geometry of the assembly, an actual half section view of a typical finished product is presented in Figure 4c.

Moreover, the assembly procedure was inspected by analysing the relationship between the opposite cylinder reaction R and the roller tool displacement p. This relationship was obtained by measuring the values of R and p after applying an increment ΔR and before rotating the female component to deform the workpiece along a circular path. Figure 5 shows a typical relationship between R and p for $t = 1$. To ensure that the crimping operation is repeatable, some curves are superimposed in Figure 5 for different samples designed, manufactured and crimped in the same conditions. It can be seen that the four superimposed curves are very close to each other that proves the good repeatability of the assembly procedure. From an industrial point of view, this experimental curve can be also used to determine the maximum forming load that seems to be advantageous in the tool design.

After the validation of the process, attention is paid to the effect of the process and geometrical parameters in order to determine the appropriate linkage design leading to the maximum pullout force.

3.2 Effect of design parameters

The considered parameters are the process parameter (P_c) and the geometrical parameters (t and R_g). A first study is focused on analysing the effect of the crimping depth P_c for a constant preselected values of the geometrical parameters (i.e. $t = 1$ mm and $R_g = 0$ mm). Based on this first study, an appropriate value of P_c is determined. Then, a second study is focused on analysing the effect of the geometrical parameters for the determined value of P_c.

3.2.1 Effect of process parameter (P_c)

To investigate the effect of the process parameter P_c, four values of this parameter are considered (i.e. 0.6, 0.8, 1 and 1.2 mm), while the geometrical parameters are kept constant. A value of ϕ_n equal to 8 mm is selected to obtain a wall thickness t of about the unity. This value is chosen according to industrial recommendations. A value of R_g equal to 0 mm is selected to reduce the manufacturing cost of the male component. Sectional views of typical finished products are presented in Figure 6 for the different considered values of P_c.

To study the effect of P_c on the assembly strength after crimping, the load-displacement curve obtained from the pullout test is investigated. Before that, the repeatability of the pullout test is inspected. Figure 7 shows the load-displacement curves resulted from three trials of a pullout test for an assembly with P_c equal to 1 mm. It can be seen that a good repeatability of the values is obtained. The shapes of the curves are similar. That is also observed in the other cases. However, some dispersions are observed in the maximum force F_{max}. In all cases, the dispersion does not exceed 20% of the mean value.

To illustrate the effect of P_c on the load-displacement curve, four typical curves corresponding to P_c equal to

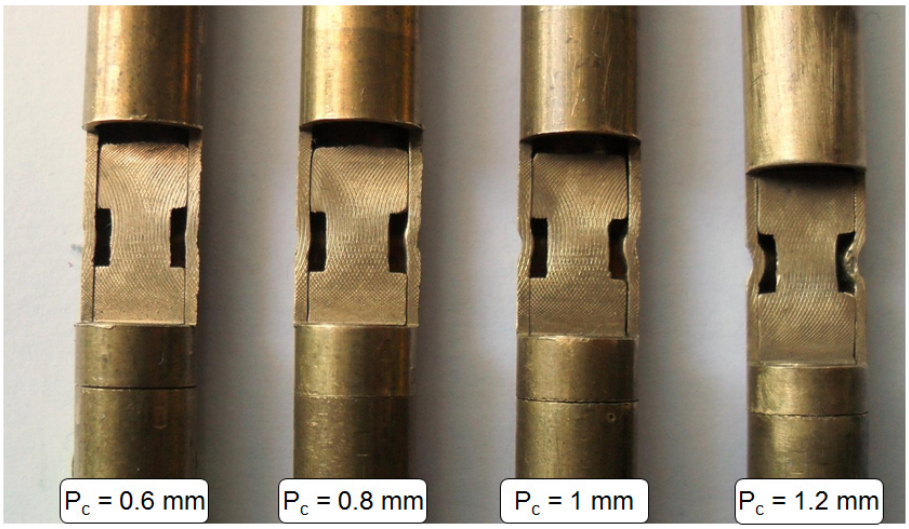

Fig. 6. Sectional views of the assembly for different values of P_c ($t = 1$ mm and $R_g = 0$ mm).

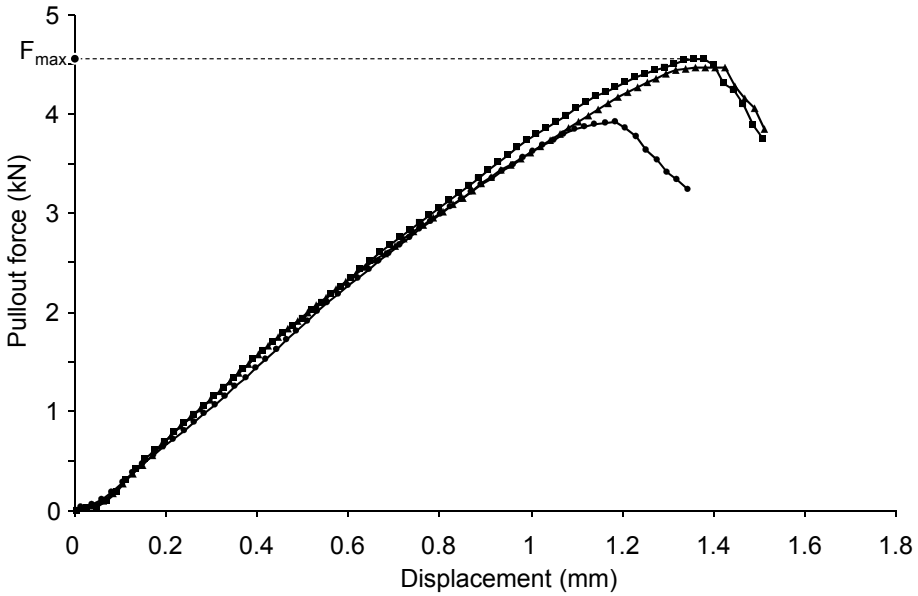

Fig. 7. The pullout force versus the displacement for three trials ($P_c = 1$ mm, $t = 1$ mm and $R_g = 0$ mm).

0.6, 0.8, 1 and 1.2 mm are plotted in Figure 8. It is clearly seen that P_c affects considerably the relationship between load and displacement in the pullout test. The assembly stiffness which corresponds to the slope at the beginning of the curve is very low for the lower values of P_c (i.e. 0.6 mm). This result indicates that in this case the crimping is at a primary stage. From P_c equal to 0.8 mm, the stiffness increases notably and becomes almost constant.

After reaching the maximum force, the assembly fails. For lower values of P_c (i.e. 0.6 mm), the male component is pulled from the female component without crack as shown in Figure 9a. However, for the other cases, an axial crack is usually observed on the outer surface of the female part as shown in Figure 9b.

To study the effect of P_c on the maximum assembly strength, the variation of F_{max} versus P_c is plotted in Figure 10. It can be seen that as P_c increases F_{max} increases. From a value of P_c equal to 1 mm, the effect of P_c on the resistance of the assembly becomes no significant. Indeed, F_{max} increases by about 2.7% when increasing P_c from 1 mm to 1.2 mm. Accordingly, a value of P_c equal to 1 mm is chosen since a higher value than the unity does not affect much the maximum assembly strength.

3.2.2 Effect of geometrical parameters

It is obvious that the reduction of the wall thickness t decreases the forming load and thus makes easier the crimping process. It also well known that a value of R_g equal to zero leads to a geometrical singularity that is undesirable in most industrial practices. Therefore, this section will focus on studying the effect of the reduction

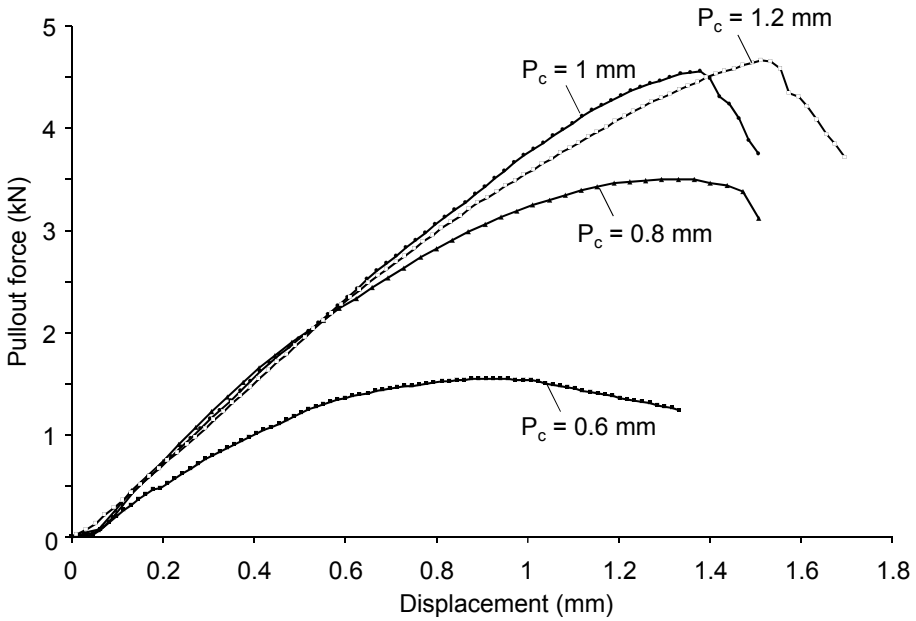

Fig. 8. The pullout force versus the displacement for different values of P_c.

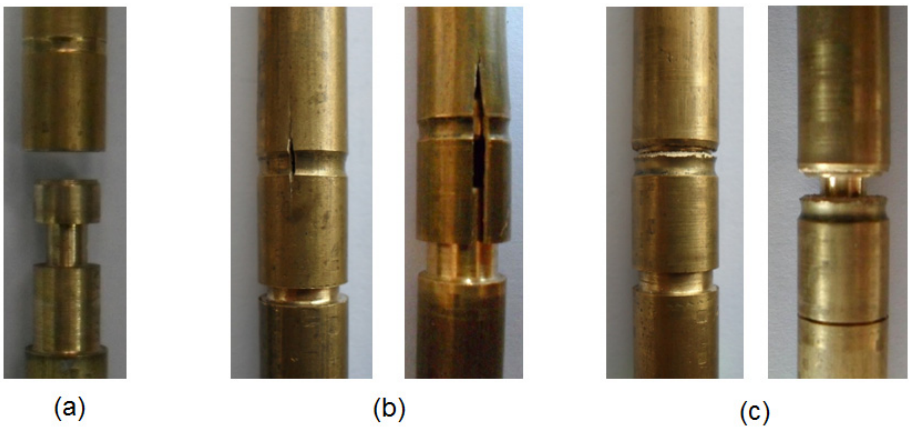

Fig. 9. Failure modes: (a) dismantling of the assembly (b) axial crack (c) radial brutal rupture.

of the wall thickness t and the effect of changing the value of the groove radius R_g. In other words, the aim is to prove or disapprove the preselected values of geometrical parameters (i.e. $t = 1$ mm and $R_g = 0$ mm).

Firstly, an assembly was designed with a wall thickness t equal to 0.75 mm. To obtain such assembly, samples were manufactured with ϕ_n equal to 8.5 mm. The other parameters were kept constant (i.e. P_c equal to the unity and R_g equal to zero). To evaluate the effect of the reduction of the wall thickness t on the forming load, a typical curve of the opposite cylinder reaction R versus the roller tool displacement p for t equal to 0.75 mm is superimposed in Figure 5. As excepted, it can be seen that the reduction of the wall thickness decreases considerably the forming load. Namely, to obtain an assembly with P_c equal to 1 mm, the forming load decreases by about 30% when the value of t decreases from 1 mm to 0.75 mm.

To illustrate the effect of the reduction of t on the pullout test results, Figure 11 shows the load-displacement curves for $t = 0.75$ mm and $t = 1$ mm. In addition to the good repeatability of the curves observed for $t = 0.75$ mm, it can be seen that t does not affect significantly the maximum strength (i.e. F_{max}). However, the assembly stiffness decreases as t decreases. It can be also noted that, for the case of t equal to 0.75 mm, a radial crack followed by a radial brutal rupture is observed as shown in Figure 9c. According to the above results, it can be concluded that the value of $t = 1$ mm can be considered as the best suited to obtain a stiffer assembly and to avoid a brutal rupture of the assembly. However, a value of $t = 0.75$ mm is more appropriate when a reduction of forming load is desired.

On the other hand, several samples were manufactured with different values of R_g (i.e. 0, 0.2, 0.5 and 1 mm). Both P_c and t were set equal to 1 mm. After performing the pullout test, the variation of F_{max} with R_g is plotted in Figure 12. It can be seen that R_g affects slightly F_{max}. Indeed, F_{max} decreases by about 7% when R_g increases from 0 mm to 1 mm. It is also found that whatever

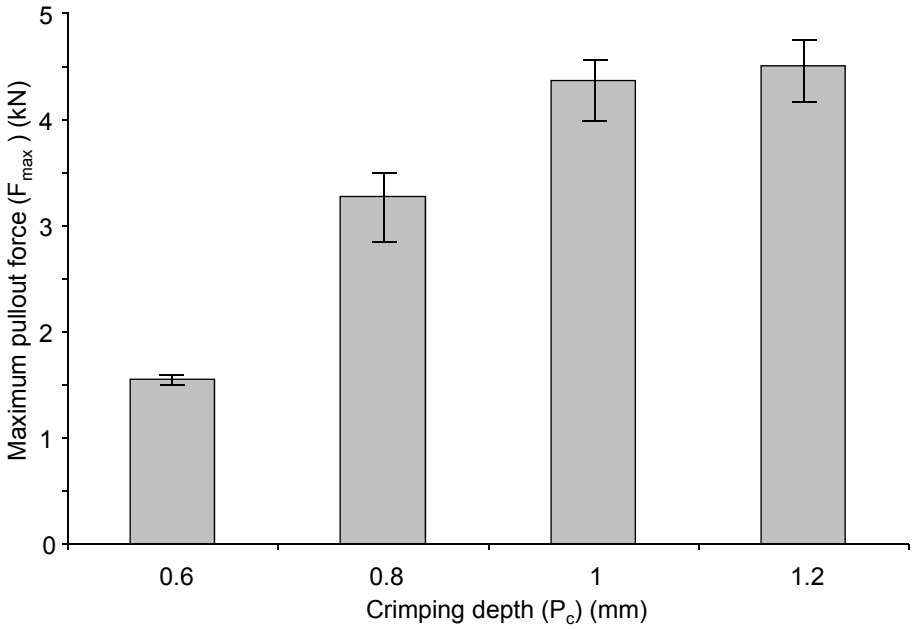

Fig. 10. Bar graph of the maximum pullout force $F_{\max}$ versus the crimping depth P_{c}.

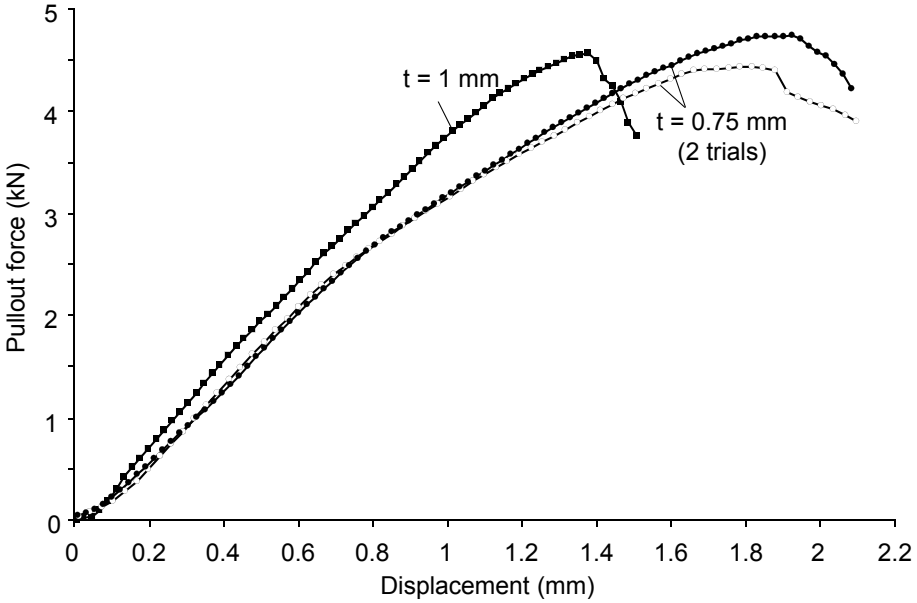

Fig. 11. The pullout force versus the displacement for different values of t.

the value of R_{g}, the assembly fails by an axial crack. It can be concluded that a value of R_{g} equal to 0 mm can be considered when a maximum assembly strength and a reduction of manufacturing cost are required. However, an appropriate value of R_{g} can be determined more accurately by testing the assembly under a rotary motion combined with an axial loading.

4 Conclusion

An assembly is designed to obtain a linkage pivot by crimping a tubular component onto a cylindrical grooved component. The assembly is manufactured by an experimental crimping device using a narrow roller tool. The analyse of the forming load during the crimping process and the final shape leads to the validation of the assembly design and processing. This validation shows that a typical revolute joint can be obtained successfully when a reduced number of components is needed.

The assembly is characterized by the means of a pullout test carried out until failure. The analysis of the results of the pullout test allows to choice the appropriate process and geometrical parameters leading to the maximum assembly strength and stiffness as well as avoiding the brutal rupture. An appropriate value of the process

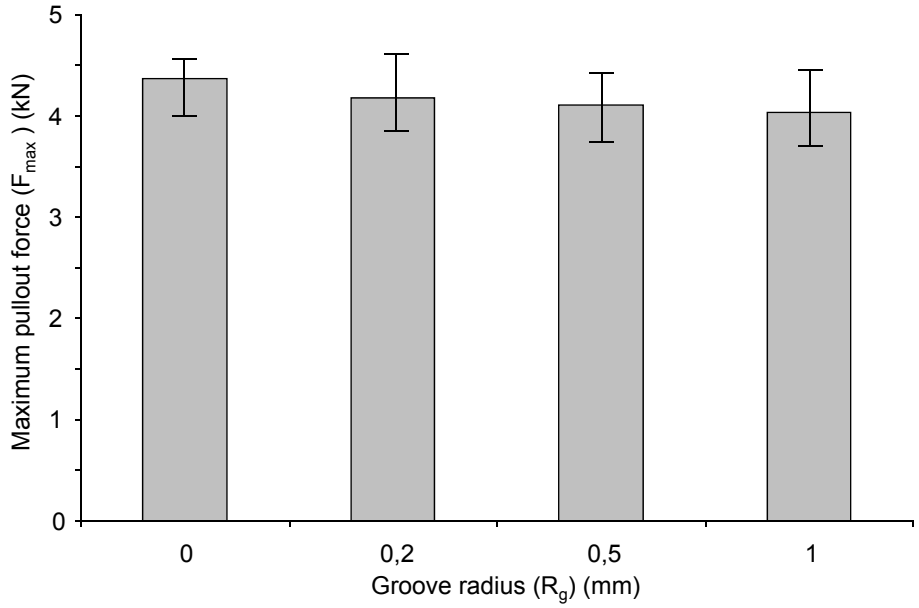

Fig. 12. Bar graph of the maximum pullout force $F_{\max}$ versus the groove radius R_{g}.

parameter (i.e. crimping depth) is determined for preselected geometrical parameters that fulfill certain industrial requirements notably the manufacturing cost. The preselected values of geometrical parameters are proved by studying the effect of a reduction of the wall thickness and the effect of changing the value of the groove radius.

Finally, it seems interesting to optimize the process and geometrical parameters by the means of a finite element model and a further characterization based on applying a rotary motion combined with an axial loading to the assembly. This will be done in future works.

References

[1] K.-I. Mori, N. Bay, L. Fratini, F. Micari, A.E. Tekkaya, Joining by plastic deformation, CIRP Annals Manuf. Technol. 62 (2013) 673–694

[2] N. Nong, O. Keju, Z. Yu, Q. Zhiyuan, T. Changcheng, L. Feipeng, Research on press joining technology for automotive metallic sheets, J. Mater. Process. Technol. 137 (2003) 159–163

[3] A.A. de Paula, M.T.P. Aguilar, A.E.M. Pertence, P.R. Cetlin, Finite element simulations of the clinch joining of metallic sheets, J. Mater. Process. Technol. 182 (2007) 352–357

[4] N. LeMaout, S. Thuillier, P.-Y. Manach, Drawing, flanging and hemming of metallic thin sheets: A multi-step process, Mater. Design 31 (2010) 2725–2736

[5] M. Shirgaokar, H. Cho, G. Ngaile, T. Altan, J.-H. Yu, J. Balconi, R. Rentfrow, W.J. Worrell, Optimization of mechanical crimping to assemble tubular components, J. Mater. Process. Technol. 146 (2004) 35–43

[6] M. Shirgaokar, G. Ngaile, T. Altan, J.-H. Yu, J. Balconi, R. Rentfrow, W.J. Worrell, Hydraulic crimping: application to the assembly of tubular components, J. Mater. Process. Technol. 146 (2004) 44–51

[7] H. Fresnel, P. Longre, V. Grolleau, P. Hardy, G. Rio, Numerical prediction of the structural failure of airbag inflators in the destructive testing phase, Eng. Failure Anal. 16 (2009) 2140–2152

[8] Y.-B. Park, H.-Y. Kim, S.-I. Oh, Design of axial/torque joint made by electromagnetic forming, Thin-Walled Structures 43 (2005) 826–844

[9] V. Psyk, D. Risch, B.L. Kinsey, A.E. Tekkaya, M. Kleiner, Electromagnetic forming a review, J. Mater. Process. Technol. 211 (2011) 787–829